



GAMMA RAY COMPUTER AIDED TOMOGRAPHY OF ADAPTIVE SCANNER SYSTEM FOR DIFFERENT TYPE AND SIZE COLUMNS.

Alex E. Moura,¹ Tiago L. Rolim¹, Carlos C. Dantas², Luis G. Charamba³, Daniel A. Vasconcelo², Silvio B. Melo³, Valdemir A. Santos⁴, Emmanuel F. Carvalho², José A. C. Silva², Rajendra Narain².

¹Department of Mechanical Engineering, ²Department of Nuclear Energy, ³Informatics Center, alexelton@gmail.com, ccd@ufpe.br -Federal University of Pernambuco – UFPE, Brazil.

⁴Department of Chemistry - Catholic University of Pernambuco – UNICAP, Brazil valdemir.alexandre@pq.cnpq.br

Abstract. A Computerized scanner set up by translation-rotation motion a 0.2 % uncertainty is measured at gamma ray trajectories sampling positions. Optimal absorption coefficient is provided by adaptive innovation design, choosing the source energy according to column material density.

Key words. Scanner design, gamma ray tomography, adaptive energy, scanner parameters.

1. INTRODUCTION

Scanner design follows an industrial requirement that involves tomography parameter as temporal resolution, instrumental radiation detector unsusceptible to magnetic fields, ambient temperature, vibration forces and maximum sensitivity for a fixed radiation energy source. Mechanical development deals with a structure to support lead shields for source and detector that realize fast and precise motion, should be simple, safe and robust. A fundamental strategy in designing the scanner is the sensitivity for the radiation source. At low energy X-ray tubes end ²⁴¹Am radioactive gamma ray source are most frequent using low atomic number materials end small dimension columns. To penetrate an industrial stain column a higher energy as ¹³⁷Cs, or ⁶⁰Co radioactive gamma sources are required.

The work is developed under the riser investigation program by gamma ray transmission measurements. Riser is a huge stain tube in FCC – Fluid Catalytic Cracking process that produces the main chemical reactions in a petroleum refinery. In gamma tomography the riser irradiation geometry is

studied by means of Beer-Lambert based equations as equations (1) and (2).

A scanner flexible geometry is described in Adaptive Design, of a single beam scanner shown in Fig. 1. Tomographic parameters are measured by means of experimental techniques developed in previous work [1], in a manual scanner. Experimental results of density, spatial and temporal resolutions in the computerized gamma ray tomography are presented under Tomography Parameters heading. These parameters evaluate the automatized system as far they are concerned. In literature, a method for linearity determination is not that easy to find, for example, in IAEA Report on Industrial Process Gamma Tomography [2], a method for linearity control using image intensity diagram along a selected line with an especial Phantom is given. Therefore, a technique based on simpler experiment and ready to quantify was investigated. At first, correlation in intensity gamma ray measurements was studied. Both results are presented under Results heading. Uncertainty evaluation and radial density distribution data are including in Results.

2. ADAPTIVE DESIGN

Innovation design provides precision, reproducibility for density distribution inside stainless as well for plexiglas columns, that are measured by choosing the gamma energy according to column wall material. Following size, column type can vary from stainless to plexiglas wall as gamma ray source of ²⁴¹Am or ⁶⁰Co can easily be installed providing adequate beam energy to penetrate scanning object.

Experiments were carried out with stainless steel tubes of 0.154 m internal diameter aim a

scale up to industrial columns, ^{137}Cs radioactive source ($7.4 \cdot 10^8$ Bq) and NaI(Tl) scintillation detector of $(51 \times 51) \cdot 10^{-3}$ m crystal size coupled to a multichannel analyzer and Genie-software from Canberra, were installed. Source and detector collimators of cylindrical aperture of $5.5 \cdot 10^{-3}$ m and $10 \cdot 10^{-3}$ m were used. the irradiation geometry source-column-detector. In a fixed alignment, it keeps a good quality gamma spectrum by means of adjusting the collimator pairs. Collimator was previously studied in [3].

The gamma ray transmission measurements were carried out by the 0.662 MeV photopeak evaluations. Compton scattering contribution was minimized by collimator length of $60 \cdot 10^{-3}$ m for source and $75 \cdot 10^{-3}$ m for detector. The scan interval $[r, r]$, with r taken according to internal radius R , was defined on the gamma profile.

The scanner design is adaptive to diameter dimension, the center of the column coincides with the origin of the Cartesian coordinates (x,y,z) , from a maximum of $(200, 200, 100)$ millimeters down to $(30, 30, 100)$ millimeters they are suitable for tomographic investigation. In Fig. 1 a stainless tube riser is fixed for scanning in source/ riser/ detector irradiation geometry.

Scanning with spatial frequency of one sample per millimeter followed by rotate one degree for the new projection angle, the uncertainty in measurement position is circa 0.2 and fairly reproducible.

A general view of the gamma ray scanner is given in Figure 1. The motion control of the CT Tomography system in Figure 1 consists of two motors and a PC. One servo-motor moves source and the detector for a parallel beam scanning, whereas the other motor rotates the column at a preset projection angle. Therefore, scanning motions and acquired data are stored and accessed by means of PC management.



Fig. 1. Gamma ray scanner

Gamma ray intensities incident and emergent I_0 and I are related with μ_L the liner attenuation coefficient by Beer-Lambert equation (1). The gamma ray tomography adapted to the riser $[x]$ proposed I_V and I_F intensities for empty and riser flow conditions, as in equation (2).

$$I = I_0 e^{-\mu_L x} \quad (1)$$

$$x = \frac{1}{\mu_L} \ln\left(\frac{I_V}{I_F}\right) \quad (2)$$

$$\rho_m = \frac{1}{\mu c} \ln\left(\frac{I_V}{I_F}\right) \quad (3)$$

In the form of equation (2) the attenuation length x is measured inside tube riser. In Equation (3), the gamma intensities are related to μ mass absorption coefficient end c is the chordal length inside riser by measuring the mean density distribution ρ_m along the gamma ray pass length.

The total absorption fraction is estimated with equation (4), it was applied for the stainless tube riser seen in Fig.1 and Plexiglas columns

$$\frac{I_0 - I}{I_0} = 1 - e^{-\mu_L x} \quad (4)$$

And using the maximal attenuation sensitivity of gamma ray given by mean path length of $\mu x = 1$; the optimal gamma ray energy was

calculated for a Plexiglas column of 100,0 mm diameter with a 0.060 MeV gamma ray from ^{241}Am . The mass attenuation coefficient evaluation by total absorption fraction value gives a 7.0 % relative error comparing with literature value [4]

3. TOMOGRAPHY PARAMETERS

To evaluate the industrial process tomography the universal criteria are:

- Spatial resolution
- Contrast or density resolution
- Temporal resolution
- Linearity

By scanning an object the number of the gamma rays trajectories and the beam width Δs : involve temporal, spatial and density resolutions as they are closely correlated parameters. Therefore, evaluation of parameters and their interaction quantification, certainly, are required in the imaging process. In order to test the CT system the tomography parameters density, spatial and temporal resolutions were measured following the techniques described in [], the data are listed in Table 1. Data are consistent and a much better reproducibility, as expected, was obtained in CT system. In single beam tomography, temporal resolution takes into account the number of projections needed for generating one image. Spatial resolution is often defined by the PSF – point spread function.

Spatial resolution was experimentally measured. The measured data described a sigmoid curve that by derivation would yield a Gaussian peak curve. Numerical derivation by means of Matlab function diff obtained the peak curve that can be seen in Fig. 2: circles are experimental data, the FWHM is indicated by the line and dashed line is the Gaussian pdf. A spatial resolution of $(6.70 \pm 0.40) \cdot 10^{-3}$ m is measured with a collimator pair of $(5.5 - 10.0) \cdot 10^{-3}$ m and a beam width of $(6.20 \pm 0.30) \cdot 10^{-3}$ m compared to a calculated point spread of $5.63 \cdot 10^{-3}$ m.

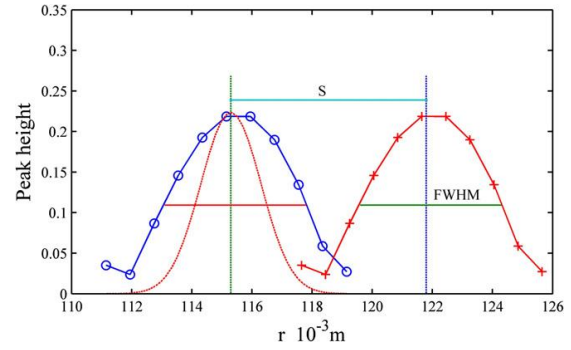


Fig. 2. Spatial resolution determination by means of the distance between peak centers $S = \text{FWHM} \cdot \sqrt{2}$.

The spatial resolution follows a criterion that is shown in Fig. 2, and values are presented in table 1. Point spread function values were calculated by the following equation

$$\text{PSF} = \frac{1}{M} [D^2 + (M-1)^2 s^2]^{1/2} \quad (5)$$

Where M is the magnification factor, D is detector collimator aperture diameter and the source size s. The gamma beam diameter is Δs and RS is the spatial resolution measurement for each Δs as it is given in Table 1.

Table 1. Measured parameters

Densidade	Espacial	Temporal
0.002g/cm ³	5 mm	2 horas
PSF	Δs	RS
5.63	3.30 ± 0.40	$3.80 \pm .60$
5.63	6.20 ± 0.30	$6.70 \pm .40$
11.15	12.00 ± 0.30	13.00 ± 0.40

Linearity is a fundamental requirement of the tomography process, as it can be observed in equation (1), by taking $\ln(I_0/I) = x \mu_L = g$, the reconstruction function will be expressed as

$$g = \int_L \mu_L(x, y) dl \quad (6)$$

Where μ_L is evaluated at point (x, y) and e L is the gamma ray path length. Further on the weight matrix W and the p vector from measured values by gamma transmission to be processed by reconstruction algorithm can be formulated in matrix notation as

$$W \mu = p \quad (7)$$

To calculate μ is necessary to solve a well known problematic [5], system of linear equations. According to [2], in tomography exists at least two different types of linearity, a) due to the path (or area) along which the integration of the attenuation property distribution take place, under this definition it is said that the tomography is not linear if the path does not follow a straight line or if it is not known and b) due to tomographic reconstruction algorithm. To evaluate reconstruction algorithm performance phantom tests are usually required. Taken into account experimental errors preliminarily, then, at algorithm evaluation would be possible to quantify uncertainty, or at least, getting an approach in this direction. In industrial tomography, each group constructs his own system following an investigation strategy. Therefore, testes for linearity of the data obtained with the system shown in Fig.1 were carried out, results are discussed.

4. RESULTS

The relation between empty/full column and flow conditions was expressed by means a criterion which applied to a large amount of data provided by CT scanner. Intensities are related in equation (2) and combined to formulates a criterion

$$\frac{\ln(I_0 / I_V)}{\ln(I_0 / I_C)} < \frac{\ln(I_V / I_F)}{\ln(I_V / I_C)} \quad (8)$$

Where, I_0 and I_C denote gamma ray intensities without tube and with full sample in tube riser, give criterion limits. Simulations by means of equations produce ideal data that were contaminate with Poisson random noise. Between limits the errors are allowed to vary and a minimum error of 2.7 % was determined.

To start with experimental data evaluation, tube riser wall thickness was measured. A stainless cylinder of (16.8 ± 0.7) cm external diameter and of (15.4 ± 0.7) cm for internal diameter. Such values are the average of five measurements by a digimatic caliper, the height standard deviations are due to irregularity in cylinder wall thickness. That effect is enhanced due to deviations from a cylinder symmetric shape. By the gamma ray profile with empty tube riser an external diameter of (16.2 ± 0.3) cm and of (15.2 ± 0.3) cm for internal diameter was graphically determined.

Linearity was investigated, using an aluminum half-moon which has known density and well defined geometry, as an experimental

tomography object. By gamma ray transmission measurement was evaluated with equation (2). The gamma ray intensities I_V , I_F are expected to be correlated since I_F is expressed in function of I_V in the exponential form of equation (2). Experimental data takes both intensities measuring twice the tube riser, then, they might also be correlated. According to correlation coefficient r given in equation:

$$r_{x,y} = \frac{\sum_{i=1}^n (x_i - \bar{x})(y_i - \bar{y})}{\sqrt{\sum_{i=1}^n (x_i - \bar{x})^2} \sqrt{\sum_{i=1}^n (y_i - \bar{y})^2}} \quad (9)$$

Experimental data shows a quite height correlation coefficient around 0.88 for the I_V and I_F intensities as aluminum half-moon measuring conditions. For centralized data the right side of the equation (9) will be replaced by the relation to calculate the angle between two vectors, as shown in equation (10), which gives the $\cos(\alpha)$, with α the angle between x and y vectors.

$$\cos(\alpha) \leq \frac{x^T x}{\|x\| \|y\|} \quad (10)$$

The matrix data $M = f(\varphi, t)$; took 12 rotation angle φ , of 15 degrees, and 97 gamma ray trajectories t , for this experiment. By means of equation (10), angle α was calculated. A least squares adjust of the correlation angle α to the rotation angle φ , is obtained and the graph in Fig. 3, shows a linear relationship with a correlation coefficient given by $R = 0.9996$, that express the explained variance of data.

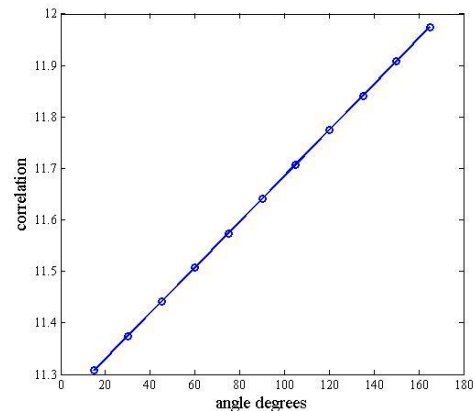


Fig. 3. Correlation and rotation angles in degrees

A second test also takes into account translation and rotation movements were performed by evaluating the attenuation length calculated with equation (2). Considering the surface area of the aluminum half-moon as

$A = \pi.R^2/2$, it can also be expressed by equation:

$$A = \int_a^b \sqrt{R^2 - z^2} dz \quad (11)$$

and will have the same area value up to two significant decimals $A = 56.55 \text{ cm}^2$. To evaluate the half-moon experiment, z will be the diameter interval $z = -6.0$: $\Delta z: 6.0$, with step $\Delta z = (b-a)/n$ and $y = \sqrt{R^2 - z^2}$, that will give objects heights around the half-moon radius $R = 6.0$ centimeters, then, the surface area A in equation (11), can be approximated by $A_n = \sum_{i=1}^n z_i y_i$, for a $n =$ sampling number.

Carrying out numerical integration using trapz a Matlab function, and $\Delta z = 0.2 \text{ mm}$, an $A_n = 56.42 \text{ cm}^2$ value is calculated. As expected with Δz smaller or, as n increases A_n will approaches A . Taken this theoretical A_n value as reference to compare with each measured $A_n(\varphi)$, from half-moon rotation angle φ , Δz as the spatial sampling frequency for the gamma ray trajectories and y as attenuation interval given by x from equation (2). The mean value from the surface areas is $\bar{A}_n = (53.3 \pm 0.6) \text{ cm}^2$; comparing with theoretical value a mean relative error of 5.6 ± 1.0 was found. with a combined standard uncertainty of 0.5992 cm^2 . This comparison may prove the half-moon area is kept constant, under experimental error limits, during angle φ rotation in gamma ray transmission measurements, according to the linear response of equation (2).

Fig. 4 displays the object at a rotation angle $\varphi = 0$ degree on top left, $\varphi = 90$ on the right.

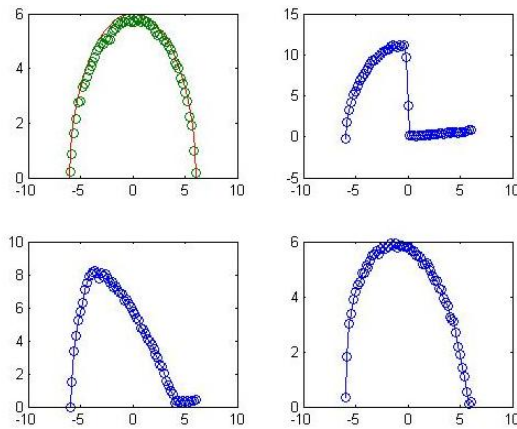


Fig. 4. Half-moon in four rotation angles

At bottom the graph shows a $\varphi = 45$ on the left and a rotation angle $\varphi = 15$ degrees on the right side is given. It can be observed that on the top left of Fig.4, for the rotation angle $\varphi = 0$, there are two graphs, experimental points in circles and a calculated line. The line describes half-moon diameter z and heights y that were used to calculated surface area A_n .

Uncertainty was carried out by means of following equation [6]:

$$u^2(y) = (\nabla_x f) V_\infty (\nabla_x f)^T \quad (12)$$

Where, $\nabla_x f$ is the sensitivity coefficient and V_∞ is the covariance matrix. Sensitive coefficients and covariance matrix were implemented by jacobian and cov Matlab functions. For the measured data calculated by equation (2), and intensity given by equation (1), uncertainty evaluation was carried out. For including the matrix covariance that describes the correlation in general the term in equation (13) was applied. As a correlated data intensities were evaluated for combined standard uncertainty, it was taken into account covariance by means of the following equation [7]:

$$u(y_1, y_m) = \sum_{i=1}^N \sum_{j=1}^N \frac{\partial y_1}{\partial x_i} \frac{\partial y_m}{\partial x_j} u(x_i) u(x_j) r(x_i, x_j) \quad (13)$$

That can describe the correlation in general expressing $y_1 = f_1(x_1, x_2, \dots, x_N)$ and

$$y_m = f_m(x_1, x_2, \dots, x_N).$$

To control gamma ray trajectories position by scanning the empty tube riser I_o and I_v intensities the tube gamma profile was measured several times, matrix data investigated by analyze of variance. Anova by Matlab functions show that no significant difference exist at same trajectory repetition by translation movement. Uncertainty evaluation on the same matrix data for I_o and I_v intensities that are not height correlated Give combined standard uncertainty by equation $u(y) = 0.0083$ and 0.0086 , values. For a correlation coefficient $r = 0.5137$; they are $u(y) = 0.0089$ and 0.0070 . By calculating combined standard uncertainty, using experimental standard given by Poisson distribution, the higher intensity value gives lower $u(y)$, as expected.

Radial density distribution of the half-moon was measured by CT scanner, and calculated with equation (3). The expected maximum

density was 1.059 g/cm^3 , at half-moon radius $R = 6 \text{ cm.}$, and minimum of 0.0879 g/cm^3 a height of 0.5 cm. The measured maximum spatial density distribution was $(1.09 \pm 0.005) \text{ g/cm}^3$, and $(0.10 \pm 0.05) \text{ g/cm}^3$ at minimum.

Results show that the errors distribution is under control. The large amount of data was obtained by measuring the flow conditions of FCC - fluidized catalyst cracking concentration distribution measured with CT scanner, data will be presented, at INAC - International Nuclear Atlantic Conference 2001, Belo Horizonte, Brazil. As expected, the highest sampling frequency gives the most accurate information about spatial distribution [2]. Tomography parameters evaluation is compared with literature data in Conclusions.

5. CONCLUSIONS

In order to give some data about the state of the art, in the Table 2, is listed tomography parameters, density spatial and temporal resolutions.

Table 2. Parameters values given in literature.

	Density g/cm^3	Spacial mm	temporal
USA	0.008	2-3	4 hs
Noruega	-	5	immediate
Alemanha	0.002	2	240 ms
França	-	-	-

The groups lieder in industrial tomography can be represented by Dudukovic M. P., from Washington University, USA; Johansen G. A. from the University of Bergen, Norway; Hampel U. from Germany, in transmission tomography, and e Legoupil S from France in emission tomography, no data is found. Such data is a non systematized set collected from several papers. Temporal resolution has been the priority in tomography generation evolution, but parameters combination also plays a role, for example, the temporal resolution given by Dudukovic M. P of 4 hs, is longer than a previous value of 2 hs, in a less developed system.

Considering the tomography parameters in Table 1, it is clear that single beam tomography is noncompetitive compared to Table 2 data, mainly upon temporal resolution. For industrial tomography process single beam is adequate for an initial investigation [9].

The adaptive CT scanner provides precise gamma ray tomography to describe radial concentration distribution. The design is suitable for study scale up process of industrial scanner.

ACKNOWLEDGMENTS

The financial support of CNPq and fellowship are greatly appreciated. The authors wish to thank Dr. Waldir Martignoni of PETROBRAS, for FCC process technical assistance and motivation.

REFERENCES

- [1] C.C. Dantas, S.B. Melo, E.F. Oliveira, F.P.M. Simões, M.G. dos Santos, V.A. dos Santos, Measurement of density distribution of a cracking catalyst in experimental riser with a sampling procedure, Nuclear Instrum. and Methods in Physics Research B 266 (2008)841–848
- [2] IAEA – International Atomic Energy Agency, Industrial Process Gamma Tomography, May, 2008
- [3] P.C.L. da Costa, C.C. Dantas, C.A.B.O. Lira, V.A. dos Santos, A Compton Filter to improve photopeak intensity evaluation in gamma ray spectra, Nucl. Instr. and Meth. B 226 (2004) 419.
- [4] H. Hubbell and [S. M. Seltzer](#) Ionizing Radiation Division, Physics Laboratory, NIST, 2010.
- [5] M. Azzi, P. Tulier, J.R. Bernard, L. Garnero, Powder Technol. 67, (1991) 27.
- [6] M G Cox, P M Harris, Uncertainty Evaluation, Best Practice Guide No.6, NPL (2004).
- [7] INMETRO, Guia para expressão da incerteza de medição, (2003).
- [8] M. Rachid, Design optimization of high speed gamma-ray Tomography, for the degree of Doctor of Philosophy in Physics, October 2009, Department of Physics and Technology, Bergen, October 2009
- [7] MELO, S. B., DANTAS, C. C., LIMA, E. A de O, SIMOES, F. P. M., OLIVEIRA, E. F. de, SANTOS, V. A. DOS, Reconstruction of radial catalyst concentration distribution in an experimental type FCC riser, Metrology and Measurement Systems. , Vol. XIII, 2007, p.137 – 148.
- [8] MELO, S. B., DANTAS, C. C., LIMA, E. A de O, SIMOES, F. P. M., OLIVEIRA, E. F. de, SANTOS, V. A. DOS, Reconstruction of radial catalyst concentration distribution in an experimental type FCC riser, Metrology and Measurement Systems. , Vol. XIII, 2007, p.137 – 148

[9] Jongbum Kim, Sunghee Jung And Jinsup Kim, A Study On Industrial Gamma Ray CT With A Single Source-Detector Pair, Nuclear Engineering And Technology, Vol.38 No.4 June 2006.